Supplemental Methods

Cell Culture, Cell lines and transgenic mice. For construction of the MMTV/cyclin D1 vector the cDNA encoding human wild-type cyclin D1 was subcloned into pMMTV-SV40Pa (p206) vector. The sequence encoding a single FLAG tag (DYKDDDDK) was introduced by PCR to create a fusion cDNA encoding FLAG-tagged cyclin D1 (FLAG-D1). This construct was prepared and injected into fertilized FVB/N mouse oocytes and implanted into pseudopregnant FVB fosters using standard methods (1). Pups were examined for successful insertion of the respective transgenes using tail genomic DNA and PCR primers for the SV40 cassette with confirmation by Southern blotting as described (1). The founder a line was called MFD1 and boasted robust levels of transgene expression in mammary tissue as determined by Northern blotting with a human cyclin D1 cDNA probe (1, 2). Tetracycline-inducible human cyclin D1 transgenic FVB mice were made at the Transgene Facility of Thomas Jefferson University. MMTV-rtTA transgenic FVB mouse were kindly provided by Dr L. Chodosh at University of Pennsylvania. MMTV-rtTA mouse were cross-mated with tet-cyclin D1 mice in order to generate a double transgenic mouse.

Mouse Study Protocol. Female MFD1 and WT mice were monitored twice weekly, up to 760 days, for the development of palpable tumors. Those developing palpable tumors were sacrificed within a week of tumor detection. Mice that died (or were sacrificed due to nonspecific ill health) without palpable tumors were counted in the non-tumor group if they survived at least 650 days. Mice developing a palpable tumor at any time up to and including 760 days were

counted in the tumor group. All lines displayed normal growth, weight, general health, mammary development, and fertility; however all mice followed for evaluation of tumor kinetics were nulliparous, to avoid potentially confounding effects of parity on development of pituitary and mammary tumors in FVB mice (3). 8-week-old tetracycline-inducible cyclin D1/rtTA bi-transgenic pregnant female mice (12 days postcoitus) were treated with doxycycline through drinking water supplementation at a final concentration of 2 mg/ml. After 7 days of doxycycline treatment, the mice were sacrificed and mammary glands taken for tissue fixation and RNA/ protein isolation. M2 FLAG antibody and cyclin D1 antibody were used to detect human cyclin D1 induction by doxycycline.

Northern Blotting. Total RNA was extracted from the right inguinal mammary gland and 10μg of RNA loaded on a 1% formaldehyde-agarose gel. The membrane was hybridized with a random-primed ^{32}P-dATP labeled probe made from the 1.4 kb EcoR1 fragment of a human cyclin D1 cDNA plasmid. The human cDNA probe detects a human transgene derived RNA of 3.4 kb. A decrease in washing stringency permits cross-hybridization to an endogenous 4.5 kb murine cyclin D1 transcript. Blots were stripped and reprobed for β-actin as a loading control.

Summary of ChIP-Seq analysis. In brief, *cyclin D1*$^{-/-}$ 3T3s transduced with MSCV-FLAG/Cyclin D1 cells were fixed with 1% formaldehyde for 15 min and quenched with 0.125 M glycine. Chromatin was isolated by adding 5-10 ml lysis buffer containing PIPES, Igepal, PMSF and Protease Inhibitor Cocktail, followed by disruption with a Dounce homogenizer. Samples were pelleted by

centrifugation and resuspended in buffer containing Na deoxycholate, SDS, and Triton X-100. Lysates were sonicated using a Misonix Sonicator 3000 equipped with a microtip in order to shear the DNA to an average length of 300-500 bp. Lysates were cleared by centrifugation and the chromatin suspensions were transferred to new tubes and stored at -80 C. To prepare Input DNA (genomic DNA), two aliquots of 10-25 ul each (approximately 1/50 of each chromatin preparation) were removed and treated with RNase for 1-2 hr at 37 C, proteinase K for 3 hr at 37 C, and 65 C heat for at least 6 hr to overnight for de-crosslinking. DNAs were purified by phenol-chloroform extraction and ethanol precipitated. Pellets were resuspended in 1/5 TE. Resulting DNAs were quantified on a Nanodrop spectrophotometer. Extrapolation to the original chromatin volume allowed determination of the yield for each chromatin preparation (as measured by the DNA content). Prior to use in ChIP, protein G agarose beads (Invitrogen) were preblocked using blocking proteins and nucleic acids for 3 hr. For each ChIP reaction, an aliquot of chromatin (20-30 ug) was precleared with 30 ul preblocked protein G agarose beads for 1-2 hr. ChIP reactions were set up using precleared chromatin and antibody (mouse IgG, anti-FLAG M2) in a buffer containing Na deoxycholate and incubated overnight at 4^{o}C. Preblocked protein G agarose beads were added and incubation at 4^{o}C was continued for another 3 hr. Agarose beads containing the immune complexes were washed two times each with a series of buffers consisting of the deoxycholate sonication buffer, high salt buffer, LiCl buffer, and TE buffer. An SDS-containing buffer was added to elute the immune complexes from the beads, and the eluents were subjected

to RNase treatment at 37 C for 20 min and proteinase K treatment at 37 C for 3 hr. Crosslinks were reversed by incubation overnight at 65 C, and ChIP DNAs were purified by phenol-chloroform extraction and ethanol precipitation.

ChIP-Sequencing (Illumina). ChIP DNA was amplified using the Illumina ChIP-Seq DNA Sample Prep Kit. In brief, DNA ends were polished and 5'-phosphorylated using T4 DNA polymerase, Klenow polymerase and T4 polynucleotide kinase. After addition of 3'-A to the ends using Klenow fragment (3'-5' exo minus), Illumina genomic adapters were ligated and the sample was size-fractionated (~250 bp) on a 2% agarose gel. After a final PCR amplification step (18 cycles, Phusion polymerase), the resulting DNA libraries were quantified and tested by QPCR at the same specific genomic regions as the original ChIP DNA to assess quality of the amplification reactions. DNA libraries were sequenced on a Genome Analyzer II. Sequences (36 nt reads) were aligned to the mouse genome (NCBI Build 37.1/mm9) using Eland (Illumina pipeline) software. Aligned sequence fragments were extended in silico at their 3'-ends to a length of 160 bp, which is the average genomic fragment length in the size selected library, and assigned to 32-nt bins along the genome. The resulting histograms were stored in BAR (Binary Analysis Results) files. Peak locations were determined using the MACS algorithm (4). These files were analyzed using Genpathway proprietary software that provides comprehensive information on genomic annotation, peak metrics and sample comparisons for all peaks (intervals). The MACs algorithm comparing cyclin D1/FLAG with IgG (cut off $p=10e^{-5}$); 3231 peaks were identified, 9 of which had a corresponding peak in the

IgG sample (using a threshold of fragment density >8). To view genomic peaks the BED files were uploaded to the Integrated Genome Browser (Affymetrix) to generate and visualize genomics regions bound by cyclin D1. Pathway analysis conducted using DAVID's Functional Annotation Clustering tool (5, 6). Annotation clusters represented using enrichment score; based on Fisher Exact P-Value

Transcription factor enrichment at ChIP-Seq intervals. In order to find the transcription factor binding sites we downloaded the latest version of the mouse genome, mm9 from July 2007 (7), from the UCSC Main Genome browser (8). We used the Galaxy Toolbox (9) to extract the 10 kb upstream of every gene in the mouse genome. In order to find all potential transcription factor binding sites we used the Jasper™ server (10) with the default parameters.

In order to assess the statistical significance of a finding a transcription factor within the interval sequences produced by the ChIP-Seq data we used a permutation test similar to the one proposed by (11). This test involves creating psuedo-random *in silico* ChIP-Seq experiments that represent a *null model*. We did this by shuffling the locations of the windows obtained by the ChIP-Seq experiment. For each shuffling we then counted the observed number of transcription factor binding sites within these random windows. The p-value for the observed frequency is a fraction of the counts from the *null model* that are greater than the observed counts.

Analysis within public microarray datasets. Samples in this dataset were classified among five canonical breast cancer subtypes, including luminal A, luminal B, normal-like, basal, and Her-2-overexpressing disease. Classification

was performed on these samples by computing their correlation against five expression profile centroids, representing each breast cancer subtype, and assigning them to the subtype with the highest corresponding correlation coefficient (12). Samples with a maximum correlation coefficient below 0.3 were considered unclassified. Kaplan-Meier curves were used to evaluate survival in the subset of classified samples that were annotated with metastasis-free survival time. The Log-rank test p-value was used to evaluate differences in survival curves among the five subtypes.

The relationship between CCND1 and CIN-associated genes was explored within the five subtypes. Gene transcript profiles representing the top 70 CIN-associated genes were median-centered and averaged to create a single-profile CIN signature. Median-centered CCND1 RMA expression versus median-centered CIN signature expression was presented on 2D-scatter plots. Within each subtype, the distribution of samples among the four quadrants around x=0 and y=0 was quantified and significance was assessed using a chi-square test.

Immunofluorescence and confocal analysis. Briefly, 3T3 cells randomly growing on collagen-coated chamber-slides were rinsed in PBS, pre-fixed for 10 sec in freshly made 4% formaldehyde, permeabilized for 5 min in PBS with 0.5% Triton X-100, and then fixed for 20 min in 4% formaldehyde. Subsequently, cells were washed in PBS and blocked in 10% boiled goat serum (Vector lab) for 1 h at room temperature. Primary antibodies, diluted in 5% boiled goat serum, were incubated overnight at 4°C. Cells were then washed in PBS with 0.05% Tween 20, incubated in secondary antibodies diluted in 5% boiled goat serum for 1 hour

at room temperature, washed again and mounted with Prolong Gold antifade reagent with DAPI (Invitrogen). Primary antibodies were diluted as follows: mouse anti–α-tubulin (DM1A, Sigma-Aldrich), diluted 1:500; rabbit-anti-γ-tubulin (Abcam), diluted 1:500 and CREST (human anti-centromere protein, Antibodies Inc.), diluted 1:500. Secondary antibodies Alexa 633 goat-anti–mouse and Alexa 568 goat-anti-rabbit (Molecular Probes) were diluted 1:500. Slides were then mounted with ProLong Gold antifade reagent with DAPI (Invitrogen).

10μm Z-stacks of single cells were collected at high magnification with a Nikon EZ1 confocal imaging system. The frequency of multipolar cells was calculated on three different experiments considering at least 60 cells per sample. Metaphase plate and spindle dimensions were analyzed with MBF imageJ software on 30 metaphase cells per sample. Data were analyzed with ChiSquare (for frequency distribution) or student test.

References

1. Wang, T.C., Cardiff, R.D., Zukerberg, L., Lees, E., Arnold, A., and Schmidt, E.V. 1994. Mammary hyperplasia and carcinoma in MMTV-cyclin D1 transgenic mice. *Nature* 369:669-671.
2. Motokura, T., Bloom, T., Kim, H.G., Jüppner, H., Ruderman, J.V., Kronenberg, H.M., and Arnold, A. 1991. A novel cyclin encoded by a *bcl1*-linked candidate oncogene. *Nature* 350:512-515.
3. Radaelli, E., Arnold, A., Papanikolaou, A., Garcia-Fernandez, R.A., Mattiello, S., Scanziani, E., and Cardiff, R.D. 2009. Mammary tumor phenotypes in wild-type aging female FVB/N mice with pituitary prolactinomas. *Veterinary pathology* 46:736-745.
4. Zhang, Y., Liu, T., Meyer, C.A., Eeckhoute, J., Johnson, D.S., Bernstein, B.E., Nusbaum, C., Myers, R.M., Brown, M., Li, W., et al. 2008. Model-based analysis of ChIP-Seq (MACS). *Genome Biol* 9:R137.
5. Huang da, W., Sherman, B.T., and Lempicki, R.A. 2009. Bioinformatics enrichment tools: paths toward the comprehensive functional analysis of large gene lists. *Nucleic acids research* 37:1-13.
6. Huang da, W., Sherman, B.T., and Lempicki, R.A. 2009. Systematic and integrative analysis of large gene lists using DAVID bioinformatics resources. *Nature protocols* 4:44-57.
7. Waterston, R.H., Lindblad-Toh, K., Birney, E., Rogers, J., Abril, J.F., Agarwal, P., Agarwala, R., Ainscough, R., Alexandersson, M., An, P., et

al. 2002. Initial sequencing and comparative analysis of the mouse genome. *Nature* 420:520-562.

8. Kent, W.J., Sugnet, C.W., Furey, T.S., Roskin, K.M., Pringle, T.H., Zahler, A.M., and Haussler, D. 2002. The human genome browser at UCSC. *Genome Res* 12:996-1006.

9. Taylor, J., Schenck, I., Blankenberg, D., and Nekrutenko, A. 2007. Using galaxy to perform large-scale interactive data analyses. *Curr Protoc Bioinformatics* Chapter 10:Unit 10 15.

10. Kel, A.E., Gossling, E., Reuter, I., Cheremushkin, E., Kel-Margoulis, O.V., and Wingender, E. 2003. MATCH: A tool for searching transcription factor binding sites in DNA sequences. *Nucleic Acids Res* 31:3576-3579.

11. Tuteja, G., White, P., Schug, J., and Kaestner, K.H. 2009. Extracting transcription factor targets from ChIP-Seq data. *Nucleic Acids Res* 37:e113.

12. Hu, Z., Fan, C., Oh, D.S., Marron, J.S., He, X., Qaqish, B.F., Livasy, C., Carey, L.A., Reynolds, E., Dressler, L., et al. 2006. The molecular portraits of breast tumors are conserved across microarray platforms. *BMC Genomics* 7:96.

Supplemental Figure Legends

Supplemental Figure 1. Analysis of cyclin D1 bound genomic regions. (A) Western blot analysis (left panel) of cyclin D1 abundance in *cyclin D1*$^{+/+}$ (4 lines), *cyclin D1*$^{-/-Control}$ (3 lines) and *cyclin D1*$^{-/-Rescue}$ (2 lines) 3T3 cells. The relative abundance of cyclin D1 normalized to glyceraldehyde-3-phosphate dehydrogenase (GAPDH) is depicted in a bar chart (right panel; values are ±SD). (B) Histogram of cyclin D1 bound region relative to transcriptional start point at -1 kb to +50 kb and (C) -2 kb to +2 kb. (D) Graphical representation of transcription factor prevalence within the interval sequences. (E) Motif alignment of those motifs predicted by MEME, a motif based sequence analysis tool. Motif prediction of intervals at -2.5 kb to -10 kb, +200 bp to +10 kb and greater than 10 kb from transcriptional start site. The CTCF invariant core sequence is present within all predicted motifs.

Supplemental Figure 2. Cyclin D1 regulates transcriptional activity of several transcription factors that are enriched at cyclin D1 associated genomic intervals. Luciferase reporter gene assays were conducted using the Myc (left panel), E2F (middle panel) and Hypoxia Responsive Element (HRE) (right panel) luciferase reporter constructs. The number of responsive elements for each construct is depicted in the reporter schematic. HEK293T cells were co-transfected with cyclin D1 (50ng). Data are mean ± SD of N=4 separate transfections.

Supplemental Figure 3. Functional annotation cluster analysis comparing cyclin D1 data sets. (A) Comparison between genes identified by ChIP-chip (~900) to

the peak intervals identified by ChIP-Seq mapped in relation to the transcriptional start (TS) site. No of peaks are labeled in red for the regions described. (B) Overlap between functional annotation clusters generated in cyclin D1 Chip-Seq compared to an existing data set generated by ChIP-ChIP. (C) Pie chart depicting 17 unique functional clusters identified by Chip-Seq. The key describes the cluster term and includes the number of genes in the term.

Supplemental Figure 4. Transcriptional, Western and ChIP analysis of cyclin D1 target genes. (A) Quantitative PCR of representative gene members of two gene ontology terms: protein catabolic process and RNA processing. Genes are as follows: F-box protein 38 (Fbxo38), DEAD (Asp-Glu-Ala-Asp) box polypeptide 46 (Ddx46), F-box and WD repeat domain containing 2 (Fbxw2), ubiquitin specific peptidase 16 (Usp16), ubiquitin specific peptidase 3 (Usp3), ubiquitin specific peptidase 38 (Usp38), DEAD (Asp-Glu-Ala-Asp) box polypeptide 20 (Ddx20), integrator complex subunit 1 (Ints1), serine/arginine-rich splicing factor 1 (Sfrs1), integrator complex subunit 4 (Ints4), splicing factor 3a, subunit 3, 60kDa (Sf3a3). Normalized expression ratio of *cyclin D1*$^{-/-Rescue}$ compared to *cyclin D1*$^{-/-Control}$ 3T3 cells (all data are mean ±SEM). (B) Western blot analysis of Aurkb abundance and its phosphorylation target H3S10 in cyclin D*1*$^{-/-Control}$ *compared cyclin D1*$^{-/-Rescue}$ cells (2 matched lines). β-Tubulin used as loading control. (C) ChIP analysis of relevant (blue) and irrelevant (red) genomic regions associated with cyclin D1 for two genes: cytoskeleton associated protein 2 (Ckap2) and centromere protein P (Cenpp). Distance from peak interval (blue circle) to

transcriptional start site is shown. Irrelevant primers were designed to sequences 1 to 2 kbp upstream of the peak interval.

Supplemental Figure 5. Enlarged representative metaphases from Spectral karyotyping (SKY) of *cyclin D1*$^{-/-}$ and *cyclin D1*$^{-/-Rescue}$ cells. (A and B) *Cyclin D1*$^{-/-}$ (P6) and *cyclin D1*$^{-/-Rescue}$ MEFs respectively (P6). (C and D) *Cyclin D1*$^{-/-Control}$ (P23) and *cyclin D1*$^{-/-Rescue}$ MEFs respectively (P23). Each panel composed of the following images: inverted 4′,6-diamidino-2-phenylindole (DAPI) image of the metaphase (top right corner), raw spectral image of the metaphase (top left) and classified metaphase of the same metaphase (lower panel).

Supplemental Figure 6. (A, B and C, D) Scatter plots depicting deletion and duplications in *cyclin D1*$^{-/-}$ (P6), *cyclin D1*$^{-/-Rescue}$ MEFs (P6) and *cyclin D1*$^{-/-Control}$ (P23), *cyclin D1*$^{-/-Rescue}$ (P23) 3T3 cells respectively; represented as number of events per cell analyzed. The mean distribution is represented as a red curve.

Supplemental Figure 7. Representative high resolution maximum Z projections of *cyclin D1*$^{-/-Control}$ and *cyclin D1*$^{-/-Rescue}$ cells immunostained for α-tubulin, γ-tubulin, CREST and DAPI. Lagging chromosomes, anaphase bridges and micronuclei were detectable in these samples compared to *cyclin D1*$^{-/-Control}$ cells (arrows). Scalebar 5 μm.

Supplemental Figure 8. A) Schematic representation of the transgenic line rtTA-*CCND1* and (B) RT-PCR for expression of the tetracyline inducible (C) Western blot demonstrating inducibilty of tet-cyclin D1 transgene assessed using anti-FLAG antibody. D) Schematic representation of the transgenic line MMTV-

CCND1. (E) Northern blot for cyclin D1 transcript in mammary glands from MMTV-cyclin D1 transgenic mice compared to wild-type FVB mice (top panel). Western blot for cyclin D1 abundance in mammary tumors derived from MMTV-cyclin D1 mice compared with wild-type mammary thoracic mammary gland (lower panel). (F) Kaplan-Meier survival curves comparing MMTV-*CCND1* and WT mice. (G) Western blot analysis (left panel) of cyclin D1 abundance in *Cyclin D1*$^{+/+}$ mammary epithelial cells compared to MMTV-*CCND1* mammary gland tumors. The relative abundance of cyclin D1 normalized to GDP dissociation inhibitor (GDI) is depicted in a bar chart (right panel; all data are ±SD).

Supplemental Table 1. Interval data from cyclin D1 associated genomic regions generated by ChIP-Seq.

Supplemental Table 2. Full list of statistically significant transcription factors found in the interval sequences bound by cyclin D1 within 2 kb of the transcriptional start site.

Supplemental Table 3. List of 47 genes bound by cyclin D1 associated with the Gene-Ontology term “Cell Division”.

Supplemental Table 4. List of genomic rearrangements detected by Spectral Karyotyping in the *cyclin D1*$^{-/-}$ MEFS (P6) and the *cyclin D1*$^{-/-}$ 3T3 cells (P23). Chr#= total number of chromosomes, Dup=duplications, del=deletions, t=non-reciprocal translocations and rcp=reciprocal translocations.

Supplemental Table 5. List of primer sequences for ChIP and QT-PCR.

Supplemental Figure 1

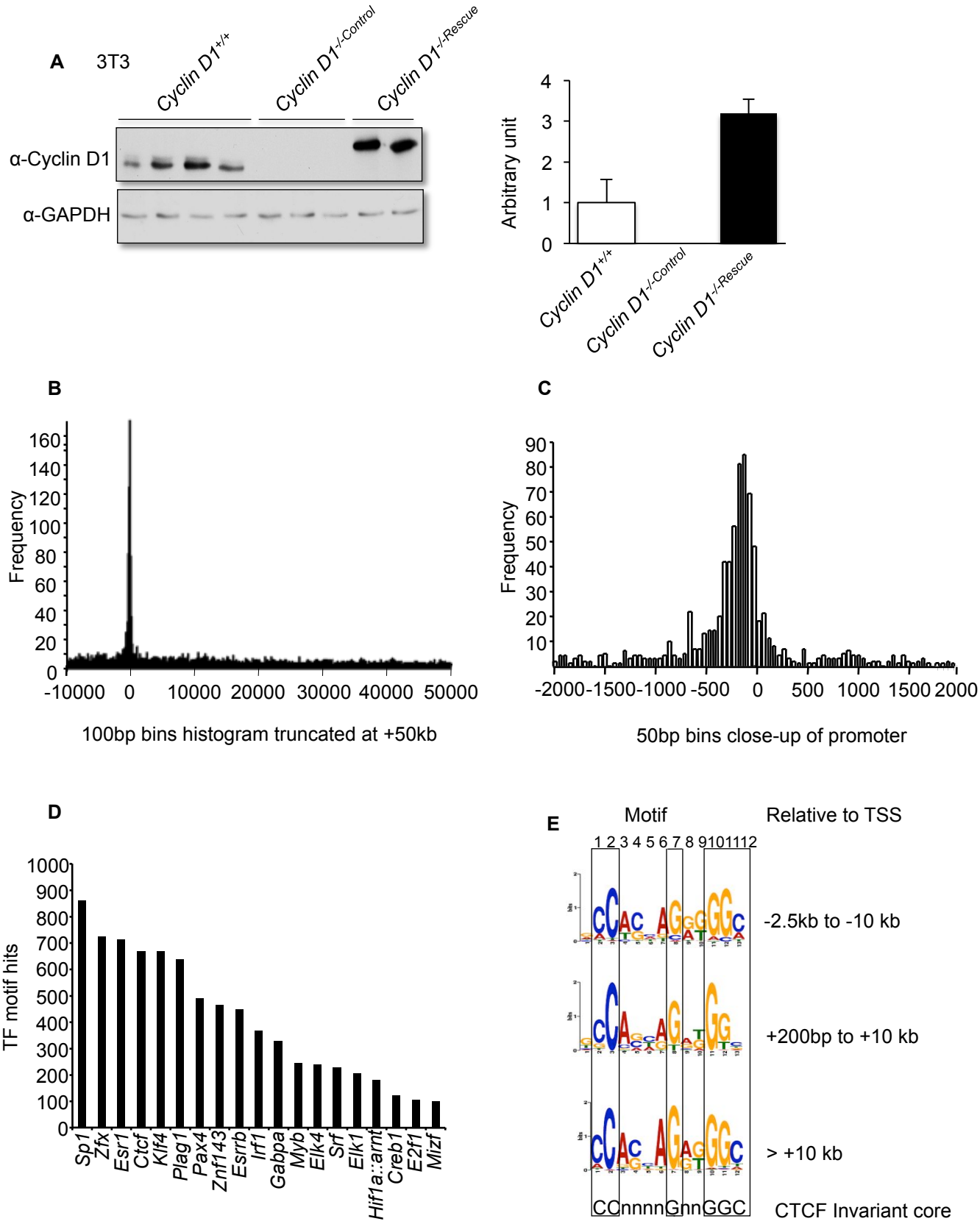

Supplemental Figure 2

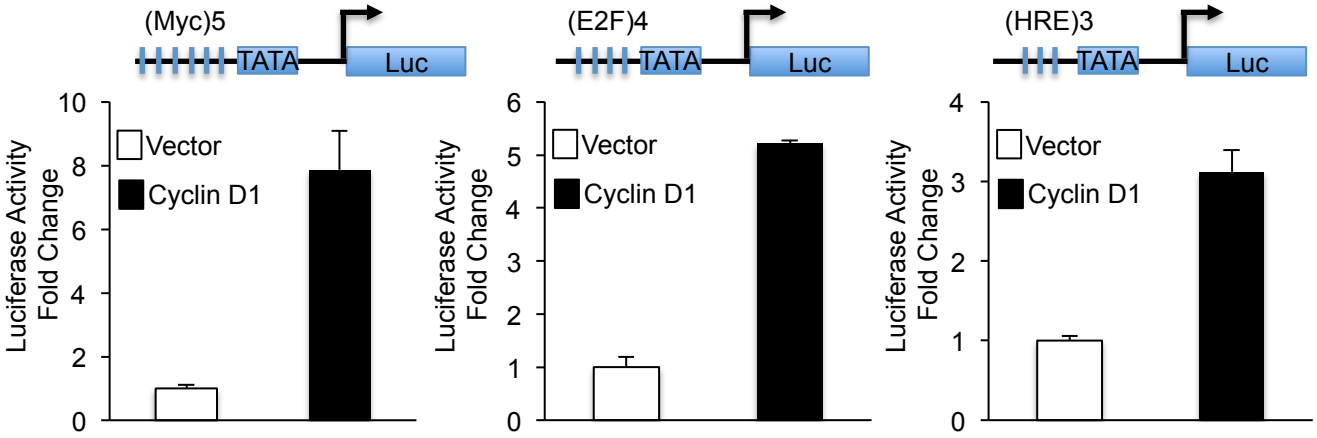

Supplemental Figure 3

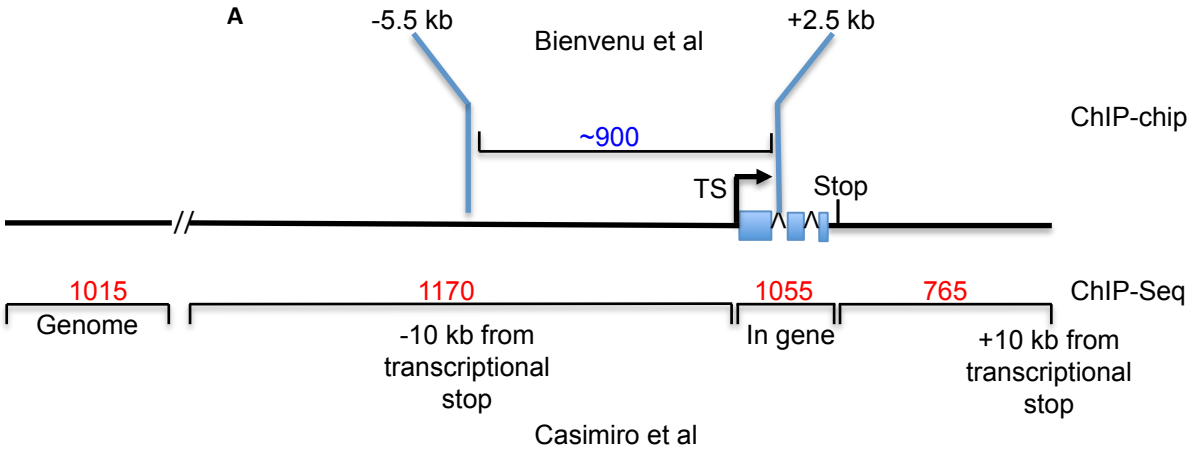

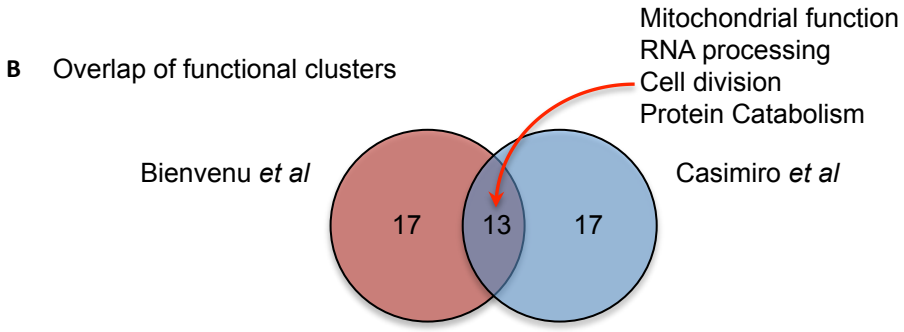

C 17 unique annotation terms in Casimiro *et al*

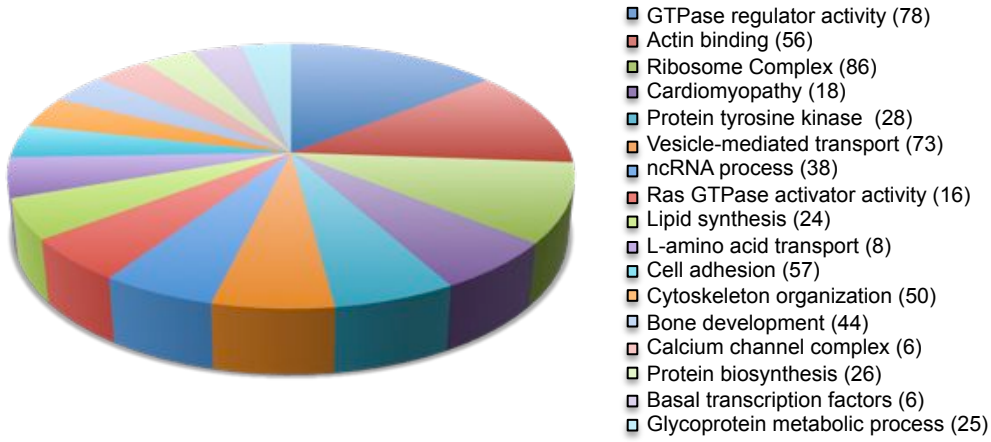

Supplemental Figure 4

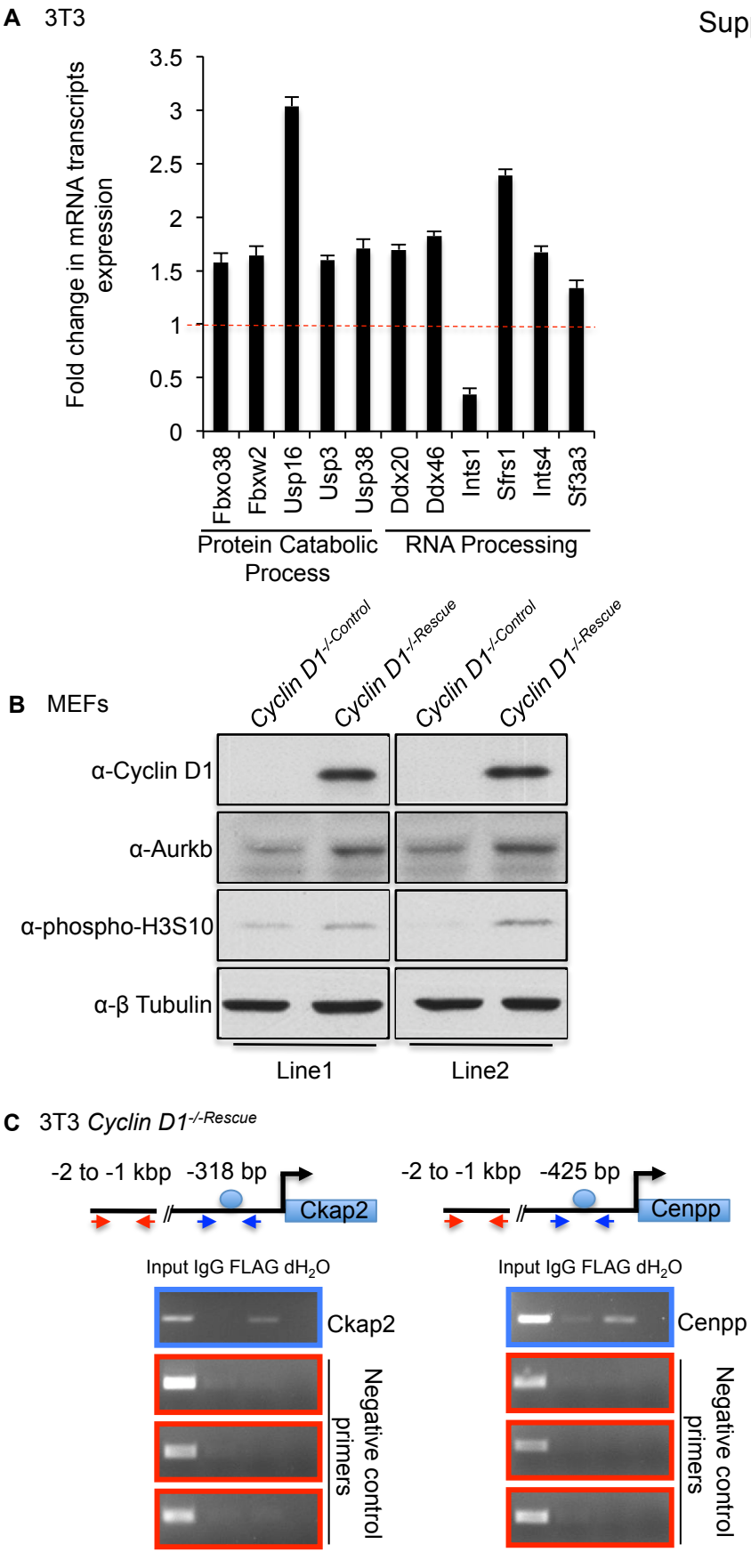

Supplemental Figure 5

A MEFS *Cyclin D1*$^{-/-}$

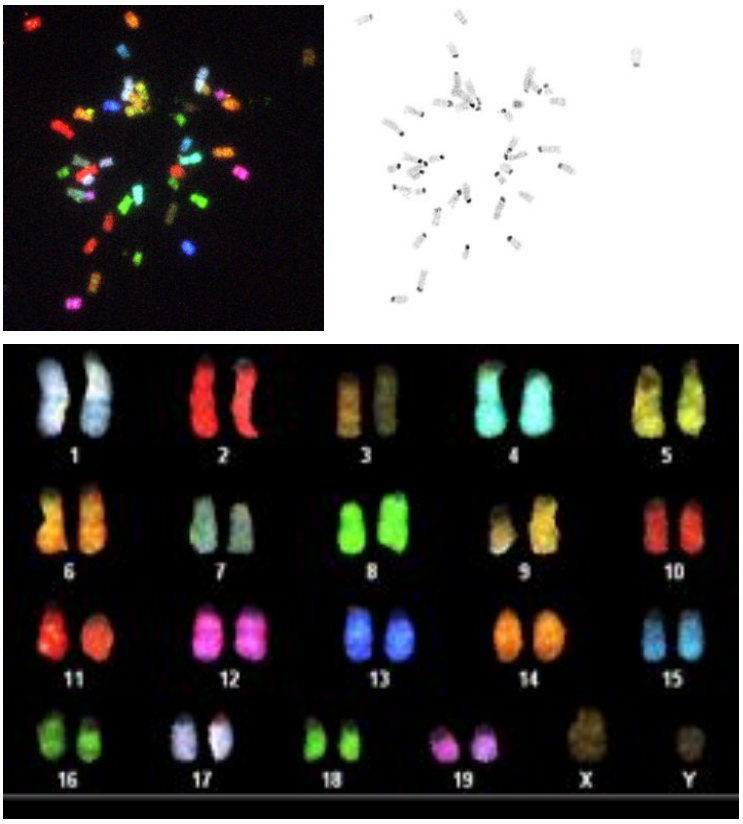

B MEFS *Cyclin D1*$^{-/-Rescue}$

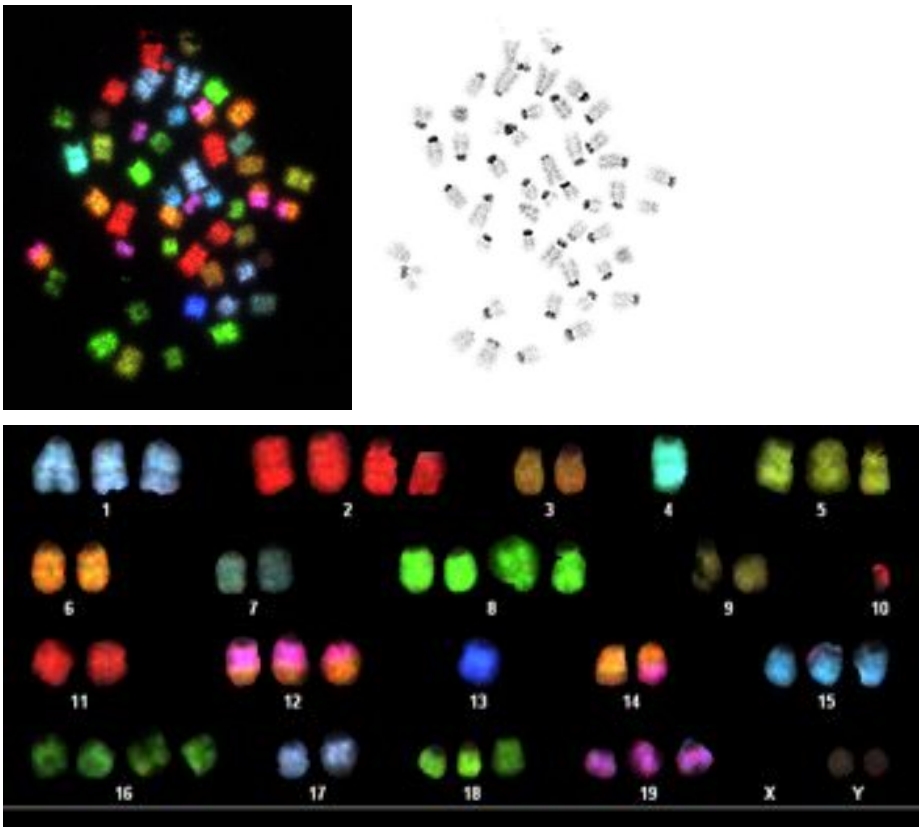

Supplemental Figure 5

C 3T3 *Cyclin D1*$^{-/-Control}$

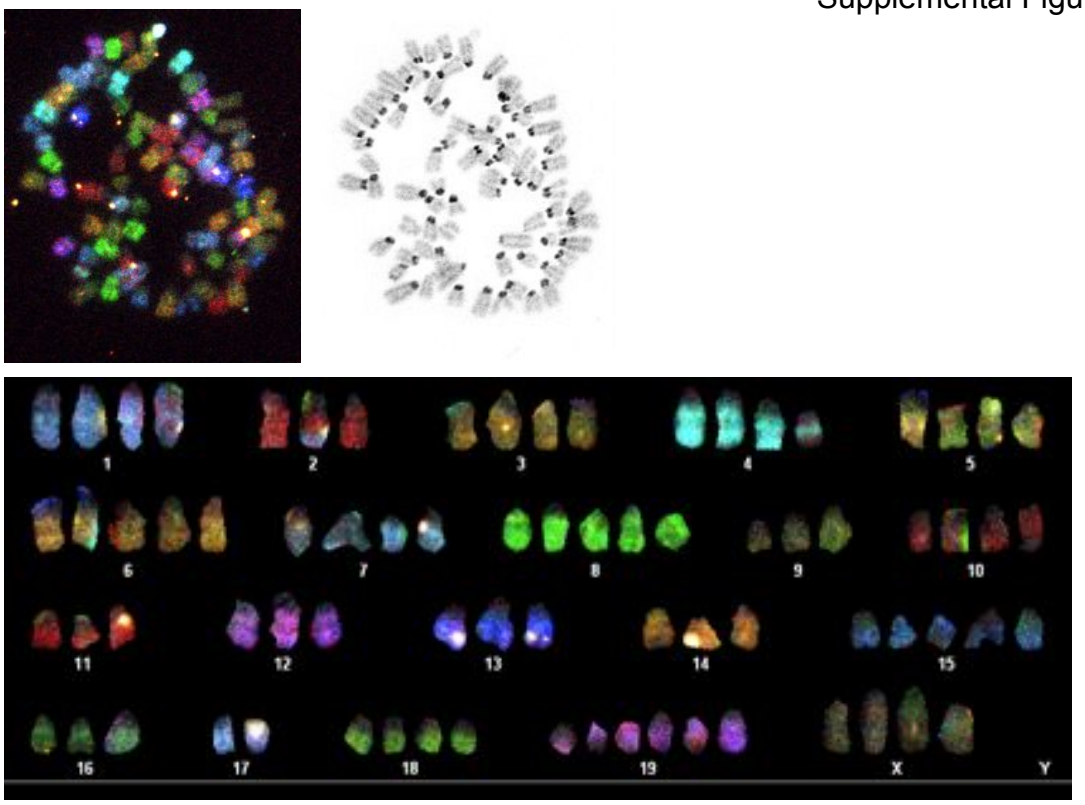

D 3T3 *Cyclin D1*$^{-/- Rescue}$

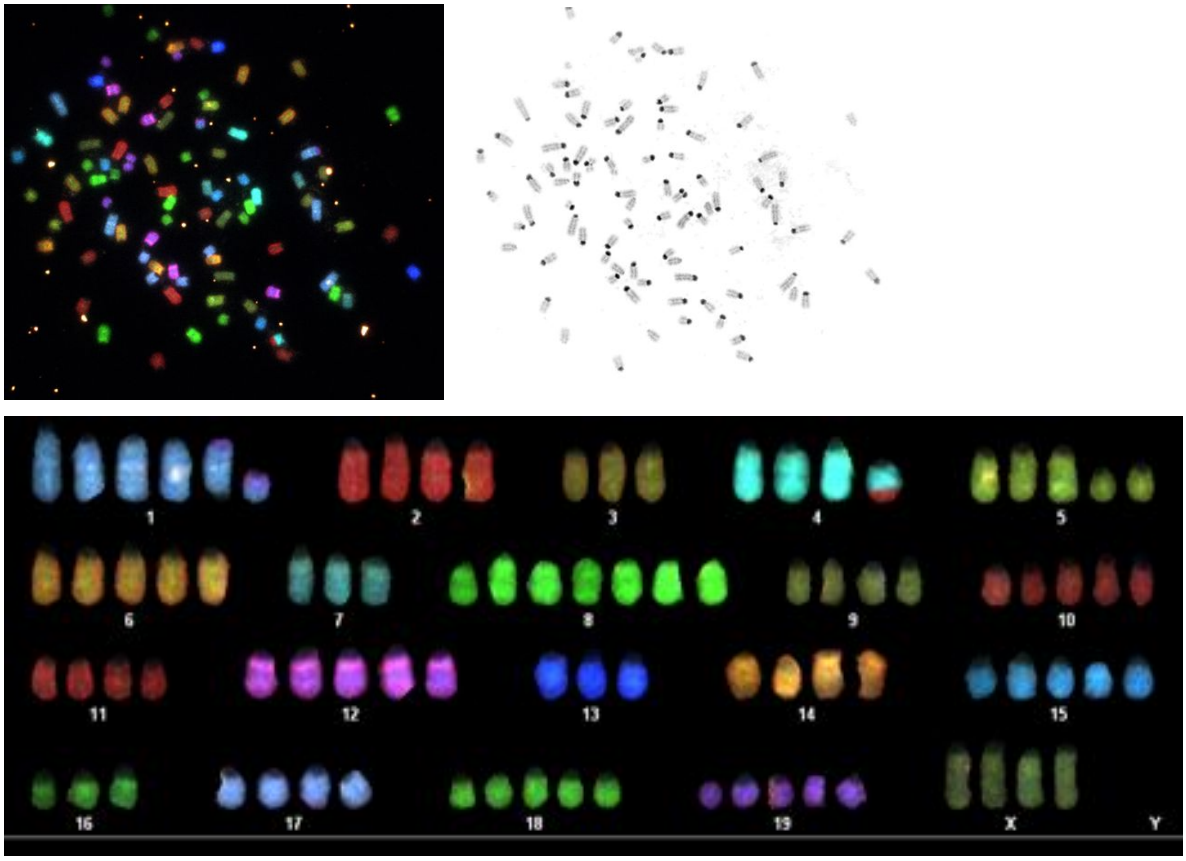

Supplemental Figure 6

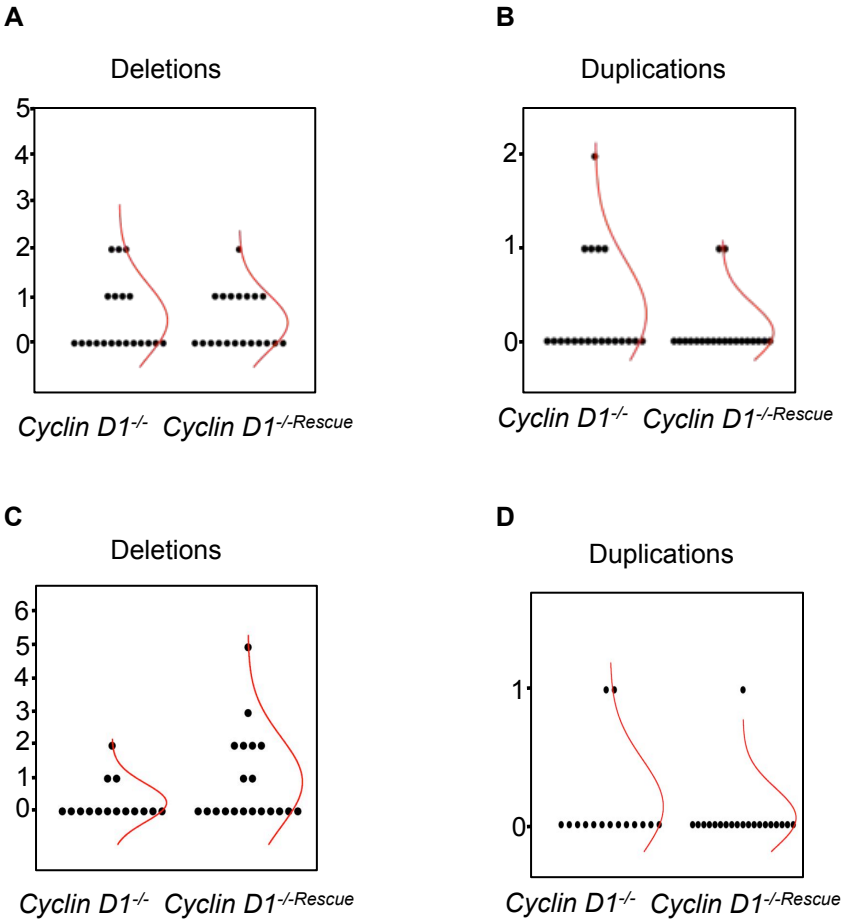

Supplemental Figure 7

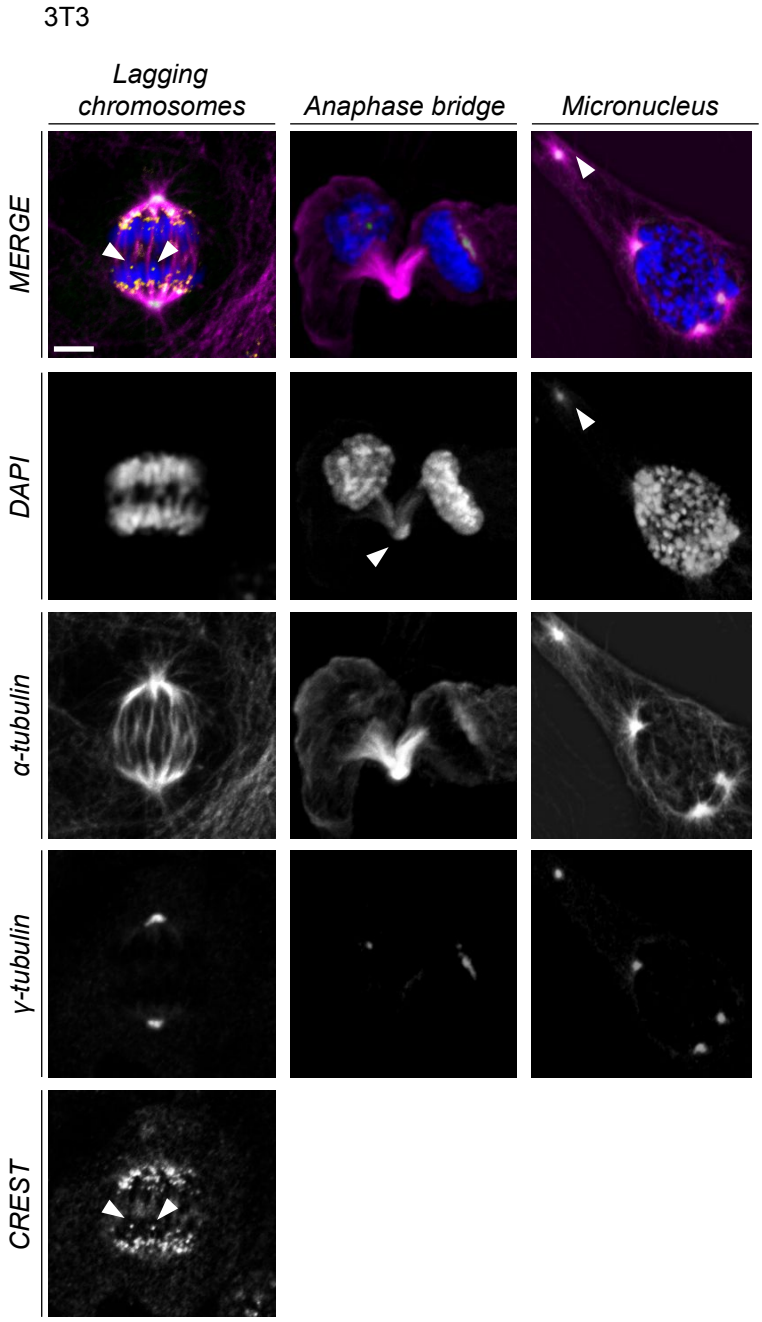

Supplemental Figure 8

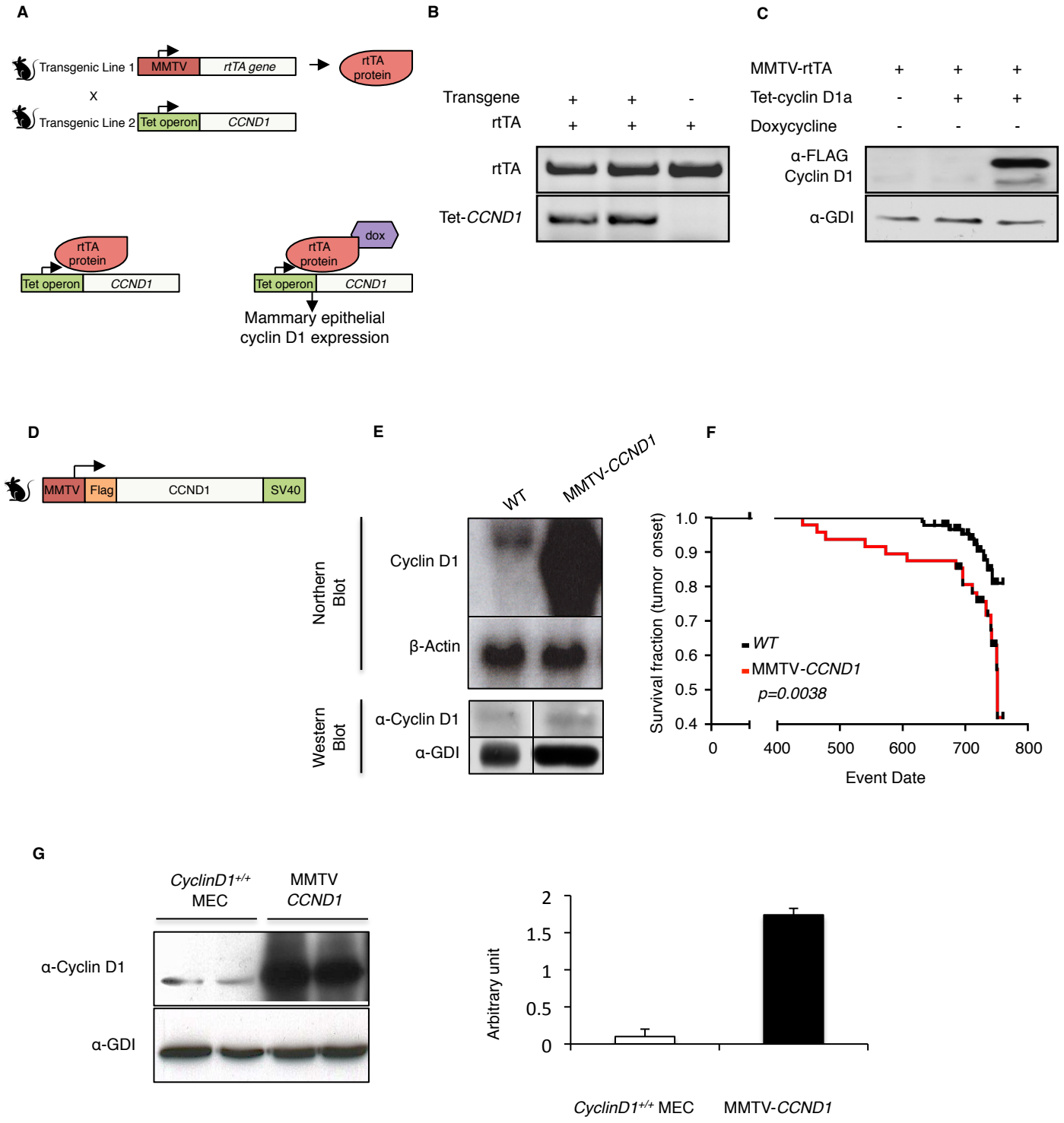

Supplemental Table 1. Interval data from cyclin D1 associated genomic regions generated by ChIP-Seq.

Description	Act Regions
Number of Intervals Converted	3222
Number of Intervals within -10000/+10000 bp of NCBI Genes	2207
Number of Intervals NOT within -10000/+10000 bp of NCBI Genes	1015
Number of NCBI Genes with Intervals within -10000/+10000 bp	2840
Number of Intervals within Promoter Region (-7500/+2500 bp of NCBI Gene Start)	986
Number of NCBI Genes with intervals in Promoters (-7500/2500 bp of start)	1313

Supplemental Table 2. Full list of transcription factor binding sites identified in cyclin D1 peak interval sequences.

Transcription factor name	P-value	Experimental hits
MA0139.1 CTCF	P<1.728e-11	670
MA0076.1 ELK4	1.728e-11	239
MA0028.1 ELK1	2.073e-05	207
MA0062.2 GABPA	2.232e-09	326
MA0163.1 PLAG1	2.282e-07	637
MA0068.1 Pax4	2.457e-05	491
MA0146.1 Zfx	4.732e-08	722
MA0079.2 SP1	4.810e-10	862
MA0131.1 MIZF	5.941e-07	100
MA0083.1 SRF	6.020e-06	228
MA0088.1 znf143	6.025e-08	466
MA0100.1 Myb	6.452e-05	244
MA0018.2 CREB1	7.588e-07	121
MA0141.1 Esrrb	8.143e-05	448
MA0112.2 ESR1	9.530e-10	713
MA0024.1 E2F1	9.685e-08	105
MA0050.1 IRF1	0.000121818	367
MA0039.2 Klf4	0.000122215	667
MA0259.1 HIF1A::ARNT	0.000146258	180
MA0116.1 Zfp423	0.000332378	533
MA0154.1 EBF1	0.000350928	519
MA0258.1 ESR2	0.000405591	520
MA0055.1 Myf	0.000694736	545
MA0117.1 Mafb	0.000894951	268
MA0060.1 NFYA	0.001173027	289
MA0099.2 AP1	0.001285588	242
MA0067.1 Pax2	0.001379599	137
MA0107.1 RELA	0.001480351	348
MA0150.1 NFE2L2	0.00179784	332
MA0162.1 Egr1	0.002145643	343
MA0158.1 HOXA5	0.002151691	114
MA0061.1 NF-kappaB	0.002239855	362
MA0038.1 Gfi	0.002353621	292
MA0059.1 MYC::MAX	0.002837581	375
MA0014.1 Pax5	0.006166234	275
MA0101.1 REL	0.006340621	317
MA0104.2 Mycn	0.007327375	333
MA0145.1 Tcfcp2l1	0.008086536	502
MA0057.1 MZF1_5-13	0.008163273	403
MA0066.1 PPARG	0.011192165	335
MA0149.1 EWSR1-FLI1	0.01137356	598
MA0003.1 TFAP2A	0.011642578	599
MA0114.1 HNF4A	0.015275332	417
MA0009.1 T	0.019976937	203
MA0111.1 Spz1	0.021119066	290
MA0140.1 Tal1::Gata1	0.023078829	208
MA0065.2 PPARG::RXRA	0.026924432	475
MA0156.1 FEV	0.02702203	215

MA0133.1 BRCA1	0.027942909	333
MA0080.2 SPI1	0.032379996	311
MA0052.1 MEF2A	0.033142678	169
MA0106.1 TP53	0.037972723	339
MA0138.2 REST	0.041318002	517
MA0030.1 FOXF2	0.045635556	193
MA0105.1 NFKB1	0.046680878	402

Supplemental Table 3. Full list of gene symbols and names associated with GeneOntology term cell division.

GO_Term Cell Division

Symbol	GENE NAME
Arl3	ADP-ribosylation factor-like 3
Cables1	CDK5 and Abl enzyme substrate 1
Clasp1	CLIP associating protein 1
Nek3	NIMA (never in mitosis gene a)-related expressed kinase 3
Nek4	NIMA (never in mitosis gene a)-related expressed kinase 4
Nek9	NIMA (never in mitosis gene a)-related expressed kinase 9
Nsl1	NSL1, MIND kinetochore complex component, homolog (S. cerevisiae)
Papd5	PAP associated domain containing 5
Racgap1	Rac GTPase-activating protein 1; predicted gene 1859
Ruvbl1	RuvB-like protein 1
Sac3d1	SAC3 domain containing 1
Setd8	SET domain containing (lysine methyltransferase) 8; predicted gene 8590
Spc25	SPC25, NDC80 kinetochore complex component, homolog (S. cerevisiae)
Zw10	ZW10 homolog (Drosophila), centromere/kinetochore protein
Anapc1	anaphase promoting complex subunit 1
Anapc2	anaphase promoting complex subunit 2
Anapc5	anaphase-promoting complex subunit 5; similar to anaphase-promoting complex subunit 5
Anln	anillin, actin binding protein
Aurkb	aurora kinase B
Bin3	bridging integrator 3
Bub1	budding uninhibited by benzimidazoles 1 homolog (S. cerevisiae)
Cdca5	cell division cycle associated 5
Cenpe	centromere protein E
Ccna2	cyclin A2
Fzr1	fizzy/cell division cycle 20 related 1 (Drosophila)
Incenp	inner centromere protein
Katnb1	katanin p80 (WD40-containing) subunit B 1
Lats2	large tumor suppressor 2
Llgl2	lethal giant larvae homolog 2 (Drosophila)
Myh9	myosin, heavy polypeptide 9, non-muscle
Pard3b	par-3 partitioning defective 3 homolog B (C. elegans)
Pard6a	par-6 (partitioning defective 6,) homolog alpha (C. elegans)
Pttg1	pituitary tumor-transforming gene 1
Cables2	predicted gene 6190; CDK5 and Abl enzyme substrate 2
Hmga2	predicted gene 7996; high mobility group AT-hook 2
Sept11	septin 11
1700017B05Rik	septin 14; RIKEN cDNA 1700017B05 gene
Sgol2	shugoshin-like 2 (S. pombe)
Cdk4	similar to Cell division protein kinase 4 (Cyclin-dependent kinase 4) (PSK-J3) (CRK3); cyclin-dependent kinase 4
Cdc14a	similar to Dual specificity protein phosphatase CDC14A (CDC14 cell division cycle 14 homolog A); CDC14 cell division cycle 14 homolog A (S. cerevisiae)
Kifc1	similar to Kifc1 protein; kinesin family member C1; predicted gene 4137
Nanog	similar to Nanog homeobox; Nanog homeobox
Nuf2	similar to Nuf2 protein; NUF2, NDC80 kinetochore complex component, homolog (S. cerevisiae)
Vps4b	similar to vacuolar protein sorting 4b; vacuolar protein sorting 4b (yeast)

Top2a	topoisomerase (DNA) II alpha
Usp16	ubiquitin specific peptidase 16
Zbtb16	zinc finger and BTB domain containing 16

Supplemental Table 4

Cell No	Chr No	Del(1)	Dup(2)	Del(3)	Dup(4)	Del(5)	t(5;19)	Dup(6)	t(6;19)	t(7;18)	Del(8)	Dup(8)	Del(16)	t(16;19)
1	60													
2	30													
3	45									1				
4	40												1	1
5	41					1	1							
6	40													
7	40													
8	80													
9	38	1												
10	81		1								1			
11	39													
12	41													
13	42											1		
14	82													
15	41													
16	31													
17	80													
18	42				1	2								
19	70	1		1	1									
20	41				1	2		1						

Cyclin D1$^{-/-}$ (p6)

Cell #	Chr #	Del(1)	t(1;3)	t(2;14)	Dic(3)	t(3;5)	t(3;7)	Dup(4)	t(4;8)	Del(5)	t(5;9)	t(5;13)	del(6)	t(8;15)	t(9;10)	del(10)	rcp(12;14)	t(12;19)	Del(13)	t(13;X)	rcp(14;12)	del(15)	t(17;19)	Del(X)
1	76																		1					
2	77					1											1							
3	34																							
4	77																		1					
5	72	1			1							1			1		3			1	1	1	1	
6	38												1											
7	76										1													
8	39																							
9	34																							
10	41							1																
11	53															1	1				1			
12	39			1				1																
13	52									1								1						
14	54																3							
15	129		1				1										3				2			1
16	49															1	3				1			
17	26																							
18	80			1										1			2				2			
19	39																							
20	35								1															

Cell #	Chr #	dup(4)	t(4;16)	ins(4;7)	del(6)	del(7)	t(8;14)	del(11)	t(11;12)	t(11;13)
1	86									
2	88							1	1	
3	85									
4	81									
5	85						1			
6	74		2							
7	71	1								
8	82					1				
9	42									
10	34									
11	48									1
12	78	1			1	1				
13	46									
14	43									
15	76			1						

Cyclin D1$^{-/-}$ (p23)

Cell #	Chr #	Del(1)	t(1;12)	t(1;19)	Del(2)	t(2;4)	Del(3)	t(3;5)	t(4;2)	t(4;18)	Del(5)	t(5;9)	t(5;15)	Del(6)	Del(7)	t(7;16)	t(7;19)	Del(8)	t(9;18)	t(8;10)	t(10;14)	Dup(11)	Del(X)	t(X;5)
1	85	1		1		1					2													
2	90															1								
3	77									1										1				1
4	83																							
5	85	1															1	1						
6	85																							
7	79							1						1										
8	94																		1					
9	150				3				2						1						1		1	
10	73								1															
11	74												1			1						1		
12	89							1																
13	95																							
14	73								1			1			1			1						
15	71																							
16	77																							
17	88		2						1		2													
18	90						1									1								
19	43																							
20	87		2						1		2													

Cyclin D1$^{-/-Rescue}$ (p23)

Supplemental Table 5. List of primer sequences for ChIP and QT-PCR.

ChIP primers

Ckap2 F	ACAAAGCTCTCCCAACTGGA
Ckap2 R	TCCAAAGATCATTCGGGAAC
Milf1ip F	AAAGGCAGGGACTCCAAACT
Milf1ip R	AGGCCGGGGAGTTCTAAAT
Zw10 F	GGGAGGGCCATAAAGGATTA
Zw10 R	GCGTCTAGAAGGCACCAAAG
Cenpp F	CTTGAACCGGAAATCAGGAA
Cenpp R	GGCAAGTGCATTTTCCTTTC
Aurkb F	GACGGGGAGAAGTGCTTTTT
Aurkb R	CCCTGCAAGGATTTCTTCTG
Top2A F	ATCACCGACTCGCTCTCATT
Top2a R	GCACATGGACCTTCCTCATT

Negative Control Primers

Ckap2 F1	TCCAGTGTTGGAATGCAGAG
Ckap2 R1	GTGTTGTCGTGGATCAGTGC
Ckap2 F2	GCACTGATCCACGACAACAC
Ckap2 R2	TGTGAACTGGCACCAGATGT
Ckap2 F3	TCAGCTTGGCTACATCTGGA
Ckap2 R3	TGAACTTGCCGATGAGAGTG
Cenpp F1	ACTGGGAGAGGACAGTCAGC
Cenpp R1	GCTTCAACTGTTGTGCCCTA
Cenpp F2	TGACCTTGCCAGAGCATATC
Cenpp R2	GCTGACTGTCCTCTCCCAGT
Cenpp F3	CAAATTGCACATGTTTTGCTTT
Cenpp R3	GCCCTGGAATCTGTCACTGT

QT-PCR primers

Ckap2 F	ATTAAGCGATGGCAGAGTCC
Ckap2 R	TTTCTTTGTTCTCGGAAGGC
Mlf1ip F	CCAGGAAACAGAAAGCTGGT
Mlf1ip R	CCTCTTCTTCCTCGAGTGCT
Zw10 F	GAAGTGCCAGGATGTGATTG
Zw10 R	AGCTTGTGATCAGCATCAGG
Cenpp F	CATGGAGATCCGCAGTACC
Cenpp R	CATCCCTTCCTCATCGATTT

Aurkb F	CCCAGAGAGTCCTACGGAAG
Aurkb R	TGTTCTCAGCCAACTTCTGG
Top2A F	ATCACCGACTCGCTCTCATT
Top2a R	GCACATGGACCTTCCTCATT
Fbxw2 F	AGTCTGCTGGTTGACTGCAC
Fbxw2 R	CCAGCCAGTTAGGGACTAGC
Fbx038 F	TCGTCCAGACCTACAAGCAG
Fbx038 R	CTCTCGGCTACCAGTTCTCC
Ddx20 F	GCAGTTTCATTGCAGAGTCC
Ddx20 R	TCACCTTCTCTGCGTCAATC
Ddx46 F	GAGTCTCGCCACTACCGAA
Ddx46 R	ACTCCTCGATCGACTTCCAG
Ints1 F	ACTCCCATGGGTCAGAAGAC
Ints1 R	GTTCCCTGATGCAGAGCATA
Ints4 F	CCAAGTGCGATTAGTGGATG
Ints4 R	AAGAGCCAAGATTGCCAAGT
Sf3a3 F	TGATGATAAGGACGGACTGC
Sf3a3 R	CACTGACATTGGCACACAGA
Sfrs1 F	ACCAGAGCCCTGATCTGTCT
Sfrs1 R	GGCAGTTTCTCCCTATTGGA
Usp3 F	GCTGCATAAATGGAGCATCA
Usp3 R	CCTCGACTCTGTCCCACATA
Usp38 F	TGGTTTACTCCCAGGTCACA
Usp38 R	TCAGCACAGTCCAGACCTTC
Usp16 F	AAACCTGAGGAGGAAGCAGA
Usp16 R	CTCGGTGTCGTGTAGTGCTT